Apoptosis-Linked Gene Product ALG-2 Is a New Member of the Calpain Small Subunit Subfamily of Ca^{2+}-Binding Proteins†

Kevin W.-H. Lo, Qiang Zhang, Ming Li, and Mingjie Zhang*

Department of Biochemistry, The Hong Kong University of Science and Technology, Clear Water Bay, Kowloon, Hong Kong, PRC

Received January 6, 1999; Revised Manuscript Received February 26, 1999

ABSTRACT: ALG-2 is a newly discovered Ca^{2+}-binding protein which has been demonstrated to be directly linked to apoptosis. Structurally, ALG-2 is expressed as a single polypeptide chain corresponding to a 22 kDa protein containing five putative EF-hand Ca^{2+}-binding sites. In this work, we have developed an efficient expression and purification scheme for recombinant ALG-2. Utilizing this protocol, we can routinely obtain purified recombinant protein with a yield of approximately 100 mg per liter of bacterial cell cultures. Gel filtration and chemical cross-linking experiments have shown that Ca^{2+}-free ALG-2 forms a weak homodimer in solution. Biochemical and spectroscopic studies of truncated and point mutants of ALG-2 demonstrated that the fifth EF-hand Ca^{2+}-binding motif is likely to participate in the formation of the dimer complex. Experimentally, both the amino- and carboxyl-terminal truncated mutants of ALG-2 have shown their ability to retain the structural, as well as, Ca^{2+}-binding integrity when individually expressed in bacteria. In this respect, the N-terminal domain encompasses the first two EF-hands, and the C-terminal domain contains the remaining three EF-hands. Combining mutagenesis and spectroscopic studies, we showed that ALG-2 possesses two strong Ca^{2+}-binding sites. Employing fluorescence spectroscopy and circular dichroism, we showed that the binding of Ca^{2+} to ALG-2 induced significant conformational changes in both the N-terminal and C-terminal domains of the protein. Furthermore, our studies demonstrated that Ca^{2+} binding to both strong Ca^{2+}-binding sites of ALG-2 is required for ion-induced aggregation of the protein. We also report here the expression, purification, and partial characterization of a Ca^{2+}-binding-deficient ALG-2 mutant (Glu47Ala/Glu114Ala). In light of its much decreased affinity for Ca^{2+}, this mutant could prove to be instrumental in elucidating the Ca^{2+}-mediated function of ALG-2 within the context of its cellular environment.

Apoptosis is a highly conserved and integrated cellular process which results in a well-orchestrated form of cell death. Over the past decade, numerous studies have clearly demonstrated that apoptosis represents a critical phenomenon essential for the normal development and maintenance of multicellular organisms (*1*−*4*). Core components comprising the apoptotic machineries and associated molecular mechanisms are remarkably conserved from nematodes to humans (*4*−*6*). However, differences in apoptotic pathways among various species do exist, and in general terms, it is well appreciated that in higher eukaryotes the process of cell death requires an elevated level of regulation and integration. Genetic analysis of *Caenorhabditis elegans* has resulted in the identification of two proapoptotic genes, *ced3* and *ced4*, as well as an antiapoptotic gene, *ced9* (*7*, *8*). These three genes are largely responsible for the proper control of apoptosis in nematodes. CED-3 is homologous to the known proapoptotic cysteine protease (Caspase-3) found in higher eukaryotes. Additionally, the gene Apaf1 is the mammalian counterpart of CED-4 (*2*, *5*).

The mammalian homologue of CED-9 has been identified as Bcl-2. It is an integral membrane protein located mainly on the cytoplasmic face of the mitochondrial outer membrane and endoplasmic reticulum (for a review, see ref *5*). It is likely that Bcl-2 exerts its function by modifying ion fluxes. In reconstituted lipid bilayers, Bcl-2 has been shown to function as a cation selective ion channel (*9*−*11*). The Bcl-2 channel activity is regulated by fluxes in intracellular Ca^{2+} concentrations (*12*). Overexpression of Bcl-2 prevents Ca^{2+} redistribution from endoplasmic reticulum to the mitochondria, thereby maintaining Ca^{2+} homeostasis (*13*, *14*) and preventing cells from Ca^{2+}-associated apoptosis (for a review, see ref *15*). Overexpression of Bcl-2 also potentiates the Ca^{2+} uptake properties of the mitochondria (*16*), and hence preserves the organelle's transmembrane potential (*17*, *18*).

For several decades, Ca^{2+} has been implicated for its role in the processes associated with cell death (for reviews, see refs *15* and *19*). An elevation of the cellular Ca^{2+} concentration was observed in glucocorticoid-induced apoptosis of lymphocytes (*20*), and the apoptotic effects of glucocorticoid can be mimicked by Ca^{2+} ionophores (*21*). Similarly, release of Ca^{2+} from the internal Ca^{2+} store using thapsigargin (an endoplasmic reticulum Ca^{2+}-ATPase inhibitor) also triggers cell death via apoptotic mechanisms (*22*). Ca^{2+}-associated apoptosis can be inhibited by extracellular Ca^{2+} chelators such as ethylene glycol bis(β-aminoethyl ether)-*N*,*N*,*N*′,*N*′-tetraacetic acid (EGTA) (*23*) or by the overexpression of a Ca^{2+} buffering protein known as calbindin D_{28K} (*24*).

† This work was partially supported by a grant from the Research Grant Council of Hong Kong to M.Z.

* To whom all correspondence should be addressed. Telephone: (852)-2358-8709. Fax: (852)-2358-1552. E-mail: mzhang@uxmail.ust.hk.

10.1021/bi990034n CCC: $18.00
Published on Web 05/18/1999

Although numerous insights have been made with respect to the characterization of the involvement of Ca^{2+} in apoptosis, the detailed role of the ion in these processes remains unclear. The uncertainty that exists regarding the absolute nature of the relationship of Ca^{2+} to apoptosis is largely the consequence of a lack of Ca^{2+}-dependent molecular targets which are directly associated with cell death. Identification of such targets will be vital for developing an understanding of the importance of Ca^{2+} in apoptosis.

Recently, a novel Ca^{2+}-binding protein, named apoptosis-linked gene-2 (ALG-2), was shown to be required for T cell receptor-, Fas-, and glucocorticoid-induced apoptosis (*25*). ALG-2 consists of a single polypepide chain of 191 amino acid residues possessing two canonical Ca^{2+}-binding sites (*25*; Figure 1A). The gene has been shown to be expressed in all mouse tissues with the highest expression occurring in thymus. More importantly, it is the first Ca^{2+}-binding protein shown to be directly linked to apoptosis. Depletion of ALG-2 using antisense RNA does not change the activity of Caspase-9, indicating that ALG-2 is likely to function downstream of the Caspase family of proteases (*26*). The expression of *ALG-2* in T cell hybridoma is not regulated by apoptosis stimuli (*25*), suggesting that the apoptotic function of ALG-2 is likely to be regulated by Ca^{2+} binding to the protein. The Ca^{2+}-dependent function of ALG-2 is consistent with the observation that the cytoplasmic Ca^{2+} level is elevated in apoptotic cells (for a review, see ref *15*).

Currently, little data pertaining to the physical and biochemical properties of ALG-2 exists. Deficiencies in such structural and functional information hamper the discernment of ALG-2 inherent regulatory and signaling characteristics as they apply to the processes of apoptosis. In this report, we describe in detail novel purification methods for the large-scale isolation of recombinant ALG-2 and several mutant forms of the protein which have been successfully expressed in bacterial cells. A number of biochemical and biophysical approaches have been used to provide evidence that ALG-2 is a member of the calpain small subunit family protein which contains five EF-hand Ca^{2+}-binding sites. We have also constructed an ALG-2 mutant which is deficient in its Ca^{2+} binding capability and, thus, makes the mutant particularly engaging for studies aimed at elucidating the Ca^{2+} dependence of ALG-2 in apoptosis.

MATERIALS AND METHODS

Cloning, Expression, and Purification of Mouse ALG-2. The mouse ALG-2 gene was PCR[1] amplified from mouse liver cDNA using the following two primers: 5′-CAGGATCCCATATGGCTGCCACTC-3′ (coding strand) and 5′-GAAGATCTTTATACAATGCTGAAGAC-3′ (noncoding strand). The rationale for the sequences of these two primers was based on the reported mouse liver cDNA cloned by Vito et al. (*25*). The amplified *ALG-2* fragment was inserted into the *Bam*HI−*Bgl*II sites of the pET3a plasmid (Novagen). The pET3a plasmid harboring *ALG-2* was then transformed into *Escherichia coli* BL21(DE3) host cells. To express ALG-2, host cells containing the *ALG-2* plasmid construct were grown in LB medium at 37 °C until reaching an A_{600} of ≈1.0. The temperature of the bacterial culture was then lowered to 25 °C to avoid formation of inclusion bodies following the induction of ALG-2 expression. Maximal ALG-2 expression was obtained by inducing the transformed cultures with isopropyl β-D-thiogalactopyranaside (IPTG) (at a final concentration of 0.5 mM), followed by the continued incubation of the cultures for ≈12 h at 25 °C. Bacterial cells were then pelleted by centrifugation and stored at −80 °C before purification.

High-yield, efficient purification of recombinant ALG-2 was achieved by modulating the protein's sensitive solubility characteristics in response to Ca^{2+}. All purification procedures were carried out at 4 °C. Cell pellets were resuspended in 20−30 mL of lysis buffer [50 mM Tris-HCl buffer (pH 7.5) containing 2 mM EDTA, 1 mM PMSF, 1 μg/mL leupeptin, and 1 μg/mL antipain] and lysed using a French press. The lysate was centrifuged at 30000*g* for 30 min. The supernatant containing ALG-2 was recovered, and $CaCl_2$ was added to a final concentration of 3 mM. The mixture was incubated on ice for 5 min while it was being stirred, and the suspension was then subjected to centrifugation at 25000*g* for 15 min. The supernatant was discarded, and the protein pellet was resolubilized with 50 mM Tris-HCl buffer (pH 7.5) containing 2 mM EDTA. The above procedure was repeated twice, before the EDTA-solubilized protein mixture was loaded onto a DEAE-Sepharose column (Amersham Pharmacia Biotech) pre-equilibrated with 50 mM Tris-HCl buffer (pH 7.5). After extensive washing, ALG-2 was eluted with a linear gradient of 0 to 0.5 M NaCl. The fractions containing ALG-2 were pooled together and concentrated before loading onto a Sephacryl-200 gel filtration column (Amersham Pharmacia Biotech). The protein was then eluted with 50 mM Tris-HCl buffer (pH 7.5) containing 2 mM EDTA and 2 mM DTT. Pure ALG-2 was dialyzed against a 0.1% NH_4HCO_3 solution, before being lyophilized for storage.

Construction, Expression, and Purification of the Amino- and Carboxyl-Terminal Fragments of ALG-2. The N-terminal fragment of ALG-2 (ALG-2-NT) containing amino acid residues Met1−Thr93 of the native protein was constructed by PCR. In addition to the full-length ALG-2 template, the following two primers were employed in the reaction: coding strand primer 5′-CAGGATCCCATATGGCTGCCTACTA-3′ and noncoding strand primer 5′-GAGGATCCTTAGTCTGTGATATAC-3′ (Figure 1C). The PCR-amplified ALG-2-NT fragment was inserted into the *Bam*HI−*Bgl*II sites of plasmid pET14b which, upon expression of the foreign gene product in an appropriate host, encodes a His tag at the N-terminus of the recombinant protein (Novagen). The ALG-2-NT-containing plasmids were then transformed into *E. coli* BL21(DE3) cells. The cells were grown at 37 °C, and ALG-2-NT was expressed as inclusion bodies. The pelleted cells were resuspended in 50 mM Tris-HCl buffer (pH 7.5) containing 2 mM EDTA, 1 mM PMSF, 1 μg/mL leupeptin, and 1 μg/mL antipain prior to lysing using a French press. Lysing of the cells was followed by sonication of the sample in the same lysis buffer. The inclusion bodies were washed three times using buffer A [50 mM Tris-HCl buffer (pH 7.5) containing 1 M urea and 0.5% Triton X-100] and twice using

[1] Abbreviations: ALG-2-NT, amino-terminal fragment (residues 1−93) of ALG-2; ALG-2-CT, carboxyl-terminal fragment (residues 93−191) of ALG-2; CD, circular dichroism; DSG, disuccinimidyl glutarate; IPTG, isopropyl β-D-thiogalactopyranoside; PCR, polymerase chain reaction; SDS−PAGE, sodium dodecyl sulfate−polyacrylamide gel electrophoresis.

A

```
                          10         20         30         40         50         60
mouse ALG-2       MAAYSYRPGP GGG----PGP AAGAA----- ---------- --LPD----- QSFLWNVFQR
human ALG-2       MAAYSYRPGP GAG----PGP AAGAA----- ---------- --LPD----- QSFLWNVFQR
human sorcin      MAYPGHPGAG GGY---YPGG YGGAP----- --------GG PAFP---GQT QDPLYGYFAA
human grancalcin  MAYPGYGGGF GNFSIQVPGM QMGQPVPETG PAILLDGYSG PAYSDTYSSA GDSVYTYFSA
porcine calpain   ---------- ---------- ---------- ---------- --------EE VRQFRRLFAQ
                                                                                *

                          70   ~     80         90         100        110        120
mouse ALG-2       VDKDRSGVIS DNELQQALS- ------NGTW TPFNPVTVRS IISMFDRENK AGVNFSEFTG
human ALG-2       VDKDRSGVIS DTELQQALS- ------NGTW TPFNPVTVRS IISMFDRENK AGVNFSEFTG
human sorcin      VAG-QDGQID ADELQRCLTQ S---GIAGGY KPFNLETCRL MVSMLDRDMS GTMGFNEFKE
human grancalcin  VAG-QDGEVD AEELQRCLTQ S---GINGTY SPFSLETCRI MIAMLDRDHT GKMGFNAFKE
porcine calpain   LAG-DDMEVS ATELMNILNK VVTRHPDLKT DGFGIDTCRS MVAVMDSDTT GKLGFEEFKY
                  :  . .:  :.  ** . *.                *.  * *  :::::* : .. .:*. *.
                     Ca2+-Site 1                                  Ca2+-Site 2

                          130        140       ~150        160        170        180
mouse ALG-2       VWKYITDWQN VFRTYDRDNS GMIDKNELKQ ALSGFGYRLS DQFHDILIR~ FDRQGRGQIA
human ALG-2       VWKYITDWQN VFRTYDRDNS GMIDKNELKQ ALSGFGYRLS DQFHDILIRK FDRQGRGQIA
human sorcin      LWAVLNGWRQ HFISFDTDRS GTVDPQELQK ALTTMGFRLS PQAVNSIAKR YSTNGK--IT
human grancalcin  LWAALNAWKE NFMTVDQDGS GTVEHHELRQ AIGLMGYRLS PQTLTTIVKR YSKNGR--IF
porcine calpain   LWNNIKKWQA IYKQFDVDRS GTIGSSELPG AFEAAGFHLN EHLYSMIIRR YSDEGGN-MD
                  :*  :. *:   :   * * * * :   **   *:   *::*.  :    : :: :. .:*   :
                                Ca2+-Site 3                                Ca2+-Site 4

                          190        200        210        220
mouse ALG-2       FDDFIQGCIV LQRLTDIFRR YDTDQDGWIQ VSYEQYLSMV FSIV (1-191)
human ALG-2       FDDFIQGCIV LQRLTDIFRR YDTDQDGWIQ VSYEQYLSMV FSIV (1-191)
human sorcin      FDDYIACCVK LRALTDSFRR RDTAQQGVVN FPYDDFIQCV MSV- (1-198)
human grancalcin  FDDYVACCVK LRALTDFFRK RDHLQQGSAN FIYDDFLQGT MAI- (1-217)
porcine calpain   FDNFISCLVR LDAMFRAFKS LDKDGTGQIQ VNIQEWLQLT MYS- (94-266)
                  **:::   :  *  :   *:   *   *  : .  ::::. . :
                                Ca2+-Site 5
```

B

12-residue Ca^{2+}-binding loop

	X		Y		Z		-Y		-X			-Z
	1	2	3	4	5	6	7	8	9	10	11	12
Consensus amino acids	D	#	D N	#	D N S	G	#	#	D E S/T	#	#	E

C

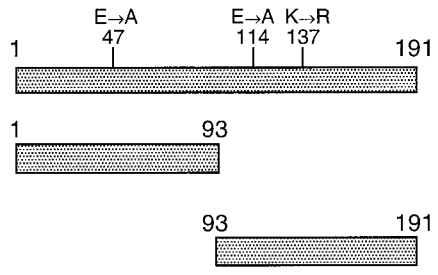

D

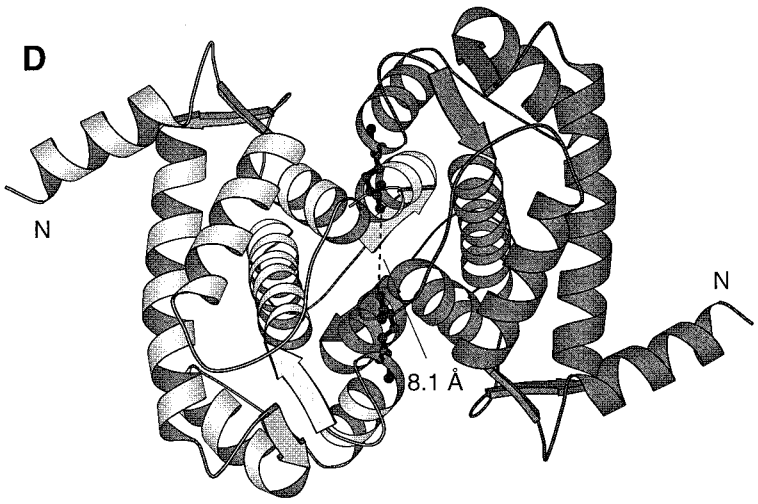

FIGURE 1: (A) Amino acid sequence alignment of ALG-2 with the other members of the calpain small subunit subfamily Ca^{2+}-binding proteins. The five Ca^{2+}-binding loops are shaded with dark boxes. The identical, highly conserved, and conserved amino acids among the sequences are denoted with *, :, and ., respectively. The positions of the point mutations used in this work are denoted with ∼. The sequence alignment was carried out using CLUSTAL W (*50*). (B) The consensus sequences of the canonical EF-hand Ca^{2+}-binding loops. (C) Schematic diagram showing the truncation and point mutations of ALG-2 created in this study. (D) Ribbon diagram showing the crystal structure of the porcine calpain symmetric dimer (PDB file name 1alv) with one monomer in light gray and the other in dark gray. The Arg214 side chain of each monomer is shown using ball-and-stick models, and the distance between the Nη of the two residues is also indicated in the figure. This figure was prepared using MOLSCRIPT (*51*).

buffer B [50 mM Tris-HCl buffer (pH 7.5) containing 1 M urea]. The purified inclusion bodies were solubilized in buffer C [20 mM Tris-HCl (pH 7.9) containing 5 mM imidazole, 0.5 M NaCl, and 6 M urea] at room temperature. The denatured protein was then passed through a Ni^{2+}−NTA affinity column using a procedure described by the manufacturer for denaturing conditions (Novagen). Refolding of ALG-2-NT was achieved by the stepwise dialysis of the denatured protein against the following buffers: (1) 0.5 M L-arginine, (2) 50 mM Tris-HCl (pH 7.5) containing 0.5 M L-arginine and 2 mM $CaCl_2$, and (3) 50 mM Tris-HCl (pH 7.5) containing 2 mM $CaCl_2$. The refolded protein was recovered from the supernatant after centrifugation, and the His tag was cleaved from the protein using thrombin (2 units of enzyme per milligram of ALG-2-NT for 4 h at room temperature). The cleaved His tag, in addition to any remaining contaminating proteins, was removed using a Sephacryl-100 gel filtration column (Amersham Pharmacia Biotech).

The C-terminal fragment of ALG-2 (ALG-2-CT) consisting of amino acids Thr93−Val191 was generated using a similar PCR-based approach as described for the generation of the ALG-2-NT mutant (Figure 1C). The PCR fragment of ALG-2-CT was inserted into pET3a. Expression of the ALG-2-CT mutant was achieved utilizing the conditions described for native ALG-2. Purification of ALG-2-CT followed a similar procedure as previously described for ALG-2 except that the $CaCl_2$ precipitation step was replaced with a 20% (w/v) ammonium sulfate fractionation.

Construction and Purification of Point Mutations of ALG-2. All point mutants of ALG-2 were generated using a PCR-based approach as previously described (*27*). Expression of the various ALG-2 point mutants in *E. coli* was identical to that described for the wild-type protein. Purification of the Lys137Arg mutant was performed using conditions identical to those described for the wild-type ALG-2. All Ca^{2+}-binding site mutants described in this work (the two single mutants Glu47Ala and Glu114Ala and the double mutant Glu47Ala/Glu114Ala) were purified using essentially the same method that was used for the wild-type ALG-2 except that the Ca^{2+}-dependent precipitation step of the protocol was substituted with a 40% ammonium sulfate fractionation step. This modification to the purification protocol as previously developed for ALG-2 is in lieu of the fact that the Ca^{2+}-binding mutants either do not bind Ca^{2+} or have very weak Ca^{2+}-binding affinity.

Chemical Cross-Linking. To cross-link free amino groups of ALG-2 as well as those of the generated truncated and point mutants of ALG-2, corresponding protein samples (0.5 mg/mL) were dissolved in 20 mM HEPES buffer (pH 8.0) containing 50 mM NaCl and 1 mM DTT. The samples were treated with 0.5 mM disuccinimidyl glutarate (DSG, Pierce) for 30 min at 25 °C. DSG was dissolved in *N*,*N*-dimethylformamide, and the final *N*,*N*-dimethylformamide concentration in the cross-linking reaction mixture was 5% (v/v). For comparison, the cross-linking reactions were carried out both in the presence and in the absence of different concentrations of Ca^{2+}.

Fluorescence Experiments. Fluorescence spectra corresponding to ALG-2 or one of the various mutants were collected on a Perkin-Elmer LS50B fluorometer in response to differing Ca^{2+} concentrations. Excitation and emission bandwidths were set at 10 and 5 nm, respectively. An excitation wavelength of 295 nm was selected for optimal observation of the intrinsic fluorescence contributed by the Trp residues of ALG-2. Emission spectra spanned wavelengths from 300 to 400 nm. The protein concentration for each of the samples was determined by the Bradford method using a commercially available assay kit (Bio-Rad).

CD Experiments. CD spectra of the wild type ALG-2 and its various mutants were measured on a JASCO J-720 CD spectropolarimeter at 25 °C. A cell path length of 1 mm was used throughout the experiments. All spectra were collected with 10 scans spanning wavelengths from 190 to 260 nm. The proteins were dissolved in 10 mM Tris-HCl (pH 7.5) containing an appropriate amount of Ca^{2+} or EDTA. The concentration of the protein samples used to collect the various CD spectra ranged from 5 to 10 μM.

RESULTS

Expression and Purification of ALG-2 and Mutant Forms of the Protein. Various expression conditions were tested as a means of optimizing the expression of ALG-2 in bacterial cells. When transformed bacterial cultures carrying a plasmid harboring the full-length sequence of ALG-2 were induced at 37 °C, the resultant recombinant protein was primarily trapped in the formation of inclusion bodies. However, when the same cultures were induced at 25 °C, essentially all of the recombinant ALG-2 was expressed as a soluble protein (Figure 2A, lane 2). Prolonged incubation of induced cultures for up to 12 h at 25 °C resulted in very high levels of expressed soluble protein (Figure 2A). During the initial stages of purification, it was discovered that ALG-2's solubility characteristics could be dramatically altered. In particular, soluble recombinant ALG-2 became almost completely insoluble when the lysis buffer was replaced with Tris-HCl buffer containing a millimolar Ca^{2+} concentration. The Ca^{2+}-induced precipitation was further demonstrated to be a reversible process following the addition of a Ca^{2+} chelator, namely, EDTA. Incorporation of this physical property into recombinant ALG-2's purification platform has significantly simplified the overall protocol. Thus, a Ca^{2+}-dependent precipitation of soluble ALG-2 is now used as the initial step of the protein's purification from bacterial lysate. Furthermore, repeated cycles of Ca^{2+} precipitation and EDTA solubilization proved to be a very efficient purification criterion, with only minor contaminating proteins remaining thereafter (Figure 2A, lane 3). These minor contaminating proteins could be effectively removed by passing the protein mixture through a DEAE-Sepharose column. The resulting recombinant ALG-2 is >95% pure and, thus, is suitable for most investigations related to its structure and function. Occasionally, protein preparations of recombinant ALG-2 were found to contain minor contaminating proteins corresponding to a molecular mass of approximately 10 kDa. These contaminating proteins could be easily removed from the preparation by gel filtration chromatography (Figure 2A). Utilizing the described purification protocol for recombinant ALG-2, we routinely obtain approximately 100 mg of purified ALG-2 from 1 L of bacterial culture grown in LB medium. The Lys137Arg point mutant of ALG-2 could be purified via the implementation of the purification protocol as described for the wild-type ALG-2. However, modification of the purification protocol

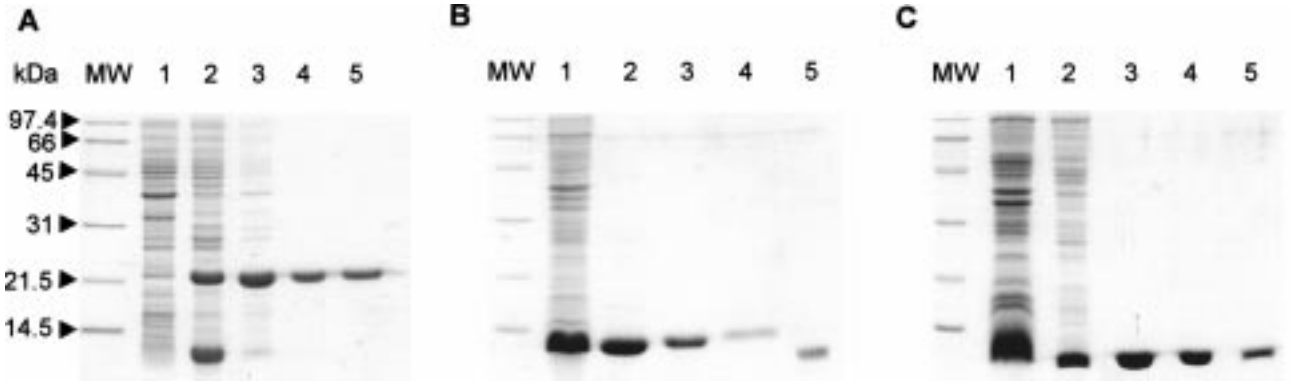

FIGURE 2: (A) Expression and purification of the full-length ALG-2 in *E. coli* cells: lanes 1 and 2, pellet and supernatant of the cell lysate, respectively; lane 3, partially purified ALG-2 after three cycles of Ca^{2+}/EDTA treatment; lane 4, ALG-2 after passage through a DEAE-Sepharose column; and lane 5, pure ALG-2 after passage through a gel filtration column. (B) Expression and refolding of ALG-2-NT from its inclusion bodies: lane 1, pellet of the ALG-2-NT-expressing cell lysate; lane 2, purification of the ALG-2-NT inclusion bodies with washing buffer containing Triton X-100 and 1 M urea; lane 3, pure, denatured His-tagged ALG-2-NT after passage through a Ni^{2+}−NTA column; lane 4, refolded, His-tagged ALG-2-NT; and lane 5, His tag-cleaved, pure ALG-2-NT after passage through a gel filtration column. (C) Expression and purification of ALG-2-CT: lanes 1 and 2, pellet and supernatant of the ALG-2-CT-expressing cell lysate, respectively; lane 3, ALG-2-CT after 20% $(NH_4)_2SO_4$ fractionation; lane 4, ALG-2-CT after passage through a DEAE-Sepharose column; and lane 5, pure ALG-2-CT after passage through a gel filtration column.

was required for the purification of all Ca^{2+}-binding site mutants of ALG-2. As a result of the mutant's weaker Ca^{2+}-binding affinities, the aforementioned Ca^{2+}-dependent precipitation step of the purification platform was replaced with a 40% (w/v) ammonium sulfate precipitation step (data not shown). The remaining steps in the purification procedures for these mutants were unaltered as compared to those employed for the wild-type ALG-2. The C-terminally truncated mutant of ALG-2 (ALG-2-NT) was constantly expressed as inclusion bodies under all test conditions employed to date. To simplify the purification protocol for the ALG-2-NT mutant, we have utilized an expression system designed to incorporate a His tag preceding the putative initiating methonine of the mutant protein's sequence. In light of the extremely high expression levels obtained with this system, substantially pure and denatured ALG-2-NT could be realized by repeatedly washing isolated inclusion bodies with a washing buffer containing 0.5% Triton X-100 and 1 M urea (Figure 2B, lane 2). Pure, denatured ALG-2-NT containing an N-terminal His tag was obtained by passing the urea-solubilized protein through a Ni^{2+}−NTA column. The mutant protein could be successfully refolded by the stepwise dialysis of the purified, His tag mutant against refolding buffers containing 0.5 M L-arginine (Figure 2B, lane 4). Through various studies, we further identified arginine and Ca^{2+} to be crucial components of the refolding buffer if efficient and high levels of refolded protein were to ensue from purified inclusion bodies of ALG-2-NT. The final yield of purified ALG-2-NT following the refolding phase of the protocol is approximately 30%. The His tag was cleaved from ALG-2-NT by thrombin and subsequently separated from the purified mutant by gel filtration chromatography (Figure 2B).

Optimal expression of a soluble form of an N-terminally truncated mutant of ALG-2 (ALG-2-CT) was achieved using expression conditions nearly identical to those reported for recombinant ALG-2. However, analogous to the Ca^{2+}-binding-deficient mutants of ALG-2, ALG-2-CT does not retain the Ca^{2+}-dependent solubility profile as observed for recombinant ALG-2. Therefore, the C-terminally truncated mutant was purified using the same procedure as that reported for the Ca^{2+}-binding-deficient mutants except that ALG-2-CT could be fractionated using 20% instead of 40% (w/v) ammonium sulfate (Figure 2C).

Ca^{2+}-Free Form of ALG-2 Exists as a Weak Dimer in Solution. Analysis of the amino acid sequence of ALG-2 revealed that the protein is highly homologous to sorcin, grancalcin, and the small subunit of calpain (Figure 1A, see the Discussion for more detail). In terms of their solution properties, sorcin, grancalcin, and the small subunit of calpain have all been reported to form homodimers (*28*−*33*). As a result, we proceeded to determine the molecular mass of recombinant ALG-2 in solution. As expected, purified recombinant ALG-2 has an apparent molecular mass of ∼22 kDa under denaturing condition as shown by SDS−PAGE (Figure 2A). In contrast to homologous proteins, ALG-2 has an apparent monomer molecular mass of ∼22 kDa in its native state and in the absence of Ca^{2+} as determined by analytical gel filtration chromatography (Figure 3A). Given its high degree of sequence identity with respect to sorcin, grancalcin, and the small subunit of calpain, it was suspected that ALG-2 may also exist as a weak dimer in solution. Since these protein−protein interactions are very weak, they cannot be detected by the method of gel filtration chromatography and require other more sensitive methods for their resolution. As a result, chemical cross-linking was used to probe the potential solution association status of ALG-2. An amine selective cross-linking reagent, DSG (with a linking spacer length of 7.7 Å), was used to probe for the formation of dimeric structure associated with recombinant ALG-2 through the cross-linking of Lys residues that possessed the appropriate accessibility and spatial orientation in solution. The high pH value of the reaction buffer and low protein concentration ensured the amine selectivity of the cross-linking reaction. SDS−PADE analysis of the cross-linking reaction clearly demonstrated the formation of a sharp band which migrated with a molecular mass of ∼44 kDa (Figure 3B, lane 1). This result supports the prediction that ALG-2, like members of its sequence-derived subfamily, exists as a weak dimer in solution in the absence of Ca^{2+}. To differentiate between specific and nonspecific cross-linking, the experiments were performed using a low concentration of cross-linker (0.5 mM

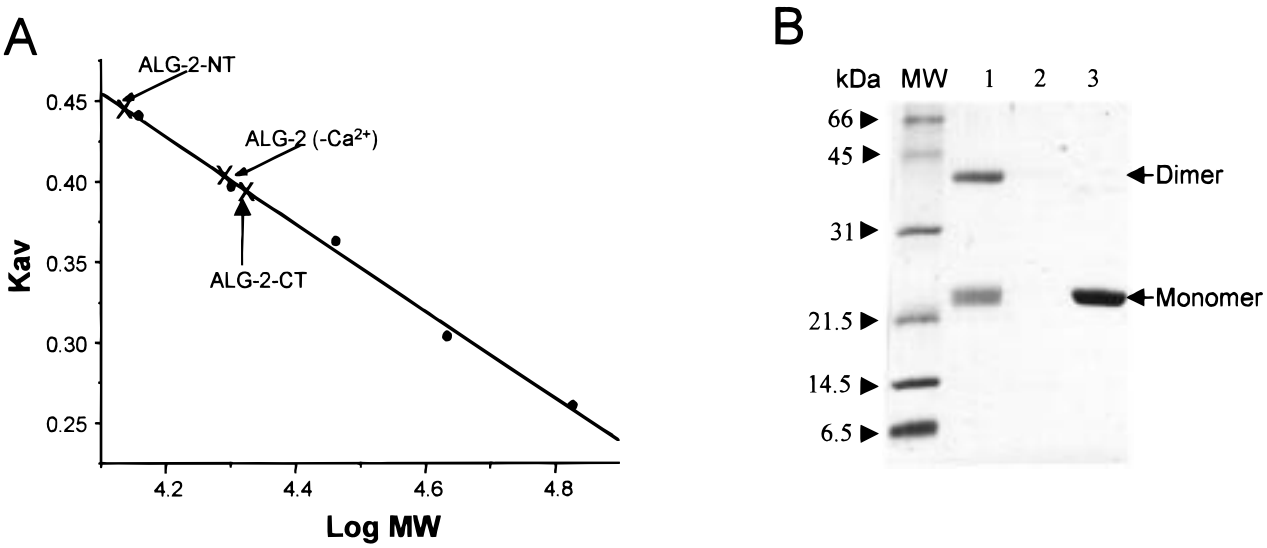

FIGURE 3: (A) Molecular mass determination of ALG-2 and its fragments by analytical gel filtration chromatography. One hundred microliters of protein sample (1 mg/mL) was injected into a Superdex 200 HR 10/30 column (Amersham Pharmacia Biotech) pre-equilibrated with 50 mM Tris-HCl (pH 7.5) containing 0.15 M NaCl and 1 mM DTT. The column was calibrated using ribonuclease A (14 kDa), trypsin inhibitor (20 kDa), carbonic anhydrase (29 kDa), ovalbumin (44 kDa), bovine serum albumin (66 kDa), and blue dextran 2000 (2000 kDa). K_{av} is defined as $(V_e - V_o)/(V_t - V_o)$, where V_e is the elution volume of a protein and V_o and V_t are the void volume and total volume of the column, respectively. (B) Chemical cross-linking of lysine residues of ALG-2 by DSG. Purified ALG-2 was treated with 0.5 mM DSG in the absence (lane 1) and presence of 1 mM Ca^{2+} (lane 2). The reactions were quenched by the addition of 0.5 M Tris-HCl (pH 7.0). The samples were resolved on a 15% SDS−PAGE gel. Purified ALG-2 serves as a control for the monomer molecular mass marker (lane 3).

DSG). Likewise, the cross-linking result remained conserved when the experiments were performed using recombinant protein concentrations as low as 0.1 mg/mL (data not shown). In contrast, if the cross-linking experiment was attempted in the presence of Ca^{2+}, the cross-linked protein complexes were incapable of migrating into the SDS−PAGE gel (Figure 3B, lane 2). The data indicate that Ca^{2+}-bound ALG-2 exists as high-molecular mass aggregates, and such aggregates can be covalently linked by DSG. We have also performed the same cross-linking reaction in the presence of micromolar concentrations of Ca^{2+}, and the same Ca^{2+}-induced aggregation was observed (data not shown). Gel filtration studies also showed that Ca^{2+}-bound ALG-2 was eluted near the void volume of the column, further supporting the observation that the Ca^{2+}-bound ALG-2 forms high-molecular mass aggregates in solution.

C-Terminal Residues Contribute to the Apparent Dimerization Potential of ALG-2. To investigate the region of the protein as well as the individual amino acids responsible for ALG-2's dimerization potential, we constructed N- and C-terminal truncation mutants using the PCR methodology. The N- and C-terminal deletion mutants were denoted ALG-2-CT and ALG-2-NT, respectively (Figure 1C). ALG-2-NT contains the first two EF-hand Ca^{2+}-binding motifs, and ALG-2-CT contains the remaining three Ca^{2+}-binding sites of the protein as predicted for all members of this sequence-derived subfamily. Both truncated mutants were capable of being obtained in a soluble, folded state as judged by their respective CD spectra (Figure 4B,C). The CD spectra are also characteristic for typical helix-rich EF-hand Ca^{2+}-binding proteins such as calmodulin. The cumulative CD spectra of the two independent truncated mutants are roughly equal to the CD spectrum of the recombinant ALG-2 (Figure 4A). These data suggest that ALG-2 consists of two separate domains.

The apparent molecular masses of both ALG-2-NT and ALG-2-CT as determined by SDS−PAGE correspond to approximately 11 kDa. The molecular mass of ALG-2-NT as measured by gel filtration is likewise approximately 11 kDa, whereas the molecular mass of ALG-2-CT as determined by gel filtration chromatography is predicted to be approximately 22 kDa (Figure 3A). These results suggest that the C-terminal fragment of ALG-2 may exist (in Ca^{2+}-free solution) as a dimer complex. Chemical cross-linking experiments further showed that ALG-2-NT failed to become cross-linked by reaction with DSG. In contrast, treatment of ALG-2-CT with DSG resulted in the formation of a dimeric complex which by the method of SDS−PAGE migrated with a corresponding molecular mass of approximately 22 kDa (Figure 5A). Taken together, these data suggest that ALG-2's dimerization region may reside within the carboxyl-terminal domain of the protein. However, one can notice that ALG-2-CT forms a much more stable dimer than the full-length protein as the full-length protein migrates as an apparent monomer in the gel filtration column. It is possible that the N-terminal domain may also modulate the solution dimerization of the protein.

We subsequently tried to locate the dimerization region of ALG-2 by identifying the Lys residue(s) that was specifically cross-linked by DSG. Inspection of the calpain small subunit crystal structure (PDB file name 1alv; *33*) suggested the side chains of Arg214 between each monomer are spatially close ($d_{N\eta-N\eta} \sim 8.1$ Å; see Figure 1D). Figure 1A shows that Lys137 of ALG-2 is aligned with Arg214 of calpain (Figure 1A), suggesting that Lys137 from each ALG-2 monomer is a likely candidate for the protein's observed cross-linking activity induced by DSG. To verify this hypothesis, we mutated Lys137 to Arg in the wild-type protein and tested the mutant's ability to dimerize. In support of the structural integrity of the mutant, CD and fluorescence

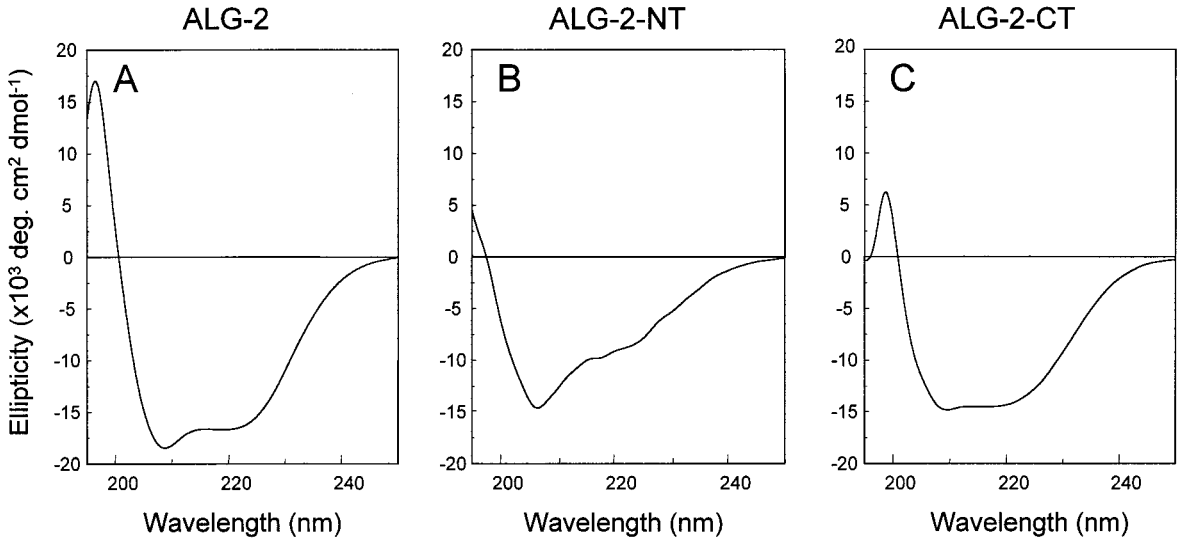

FIGURE 4: Circular dichroism spectra of Ca^{2+}-free ALG-2 (A), Ca^{2+}-bound ALG-2-NT (B), and Ca^{2+}-free ALG-2-CT (C). The protein samples were dissolved in 10 mM Tris-HCl (pH 7.5) containing 1 mM DTT and 1 mM EDTA. The concentrations of the samples were 5, 10, and 10 μM for ALG-2, ALG-2-NT, and ALG-2-CT, respectively.

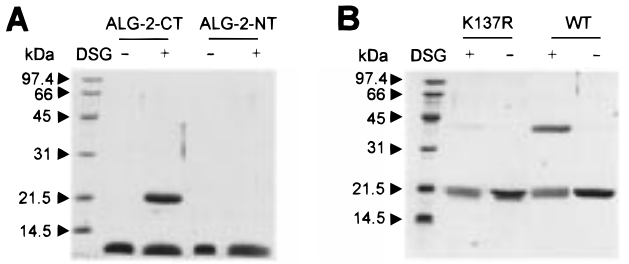

FIGURE 5: Chemical cross-linking of ALG-2-CT and ALG-2-NT (A) and the Lys137Arg mutant of ALG-2 (B) by DSG in the presence of 1 mM EDTA. The experimental details were the same as those described in the legend of Figure 3B. The wild-type ALG-2 was used as a control for comparison with the point mutation.

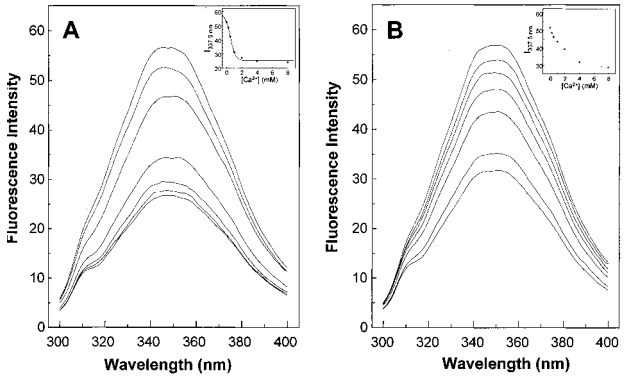

FIGURE 6: Quenching of intrinsic Trp fluorescence of full-length ALG-2 (A) and ALG-2-CT (B) with incremental amounts of added Ca^{2+}. The inset of each panel shows the decrease of fluorescence intensity at 345 nm as a function of Ca^{2+} concentration. The protein concentration was 0.01 mg/mL for both samples.

spectra confirmed that the mutant retained the same structural characteristics as those of the wild-type protein (data not shown). To determine the mutant's cross-linking capability, the Lys137Arg mutant protein was treated with DSG utilizing reaction conditions identical to those used for the wild-type protein. Figure 5B clearly demonstrates that the mutant protein no longer possesses the capacity to initiate cross-linking reactions in the presence of DSG. Furthermore, these findings related to the Lsy137Arg mutant further support previous studies which have suggested that recombinant ALG-2 dimerization potential is confined to the protein's C-terminus. In parallel studies, it was demonstrated that wild-type ALG-2 could not be successfully cross-linked by 1,5-difluoro-2,4-dinitrobenzene (another amine selective cross-linker with a space arm of ~3 Å). This finding suggests that the distance between the Nϵ of Lys137 contributed from each of the monomer is larger than 3 Å (data not shown). Collectively, these data, in addition to details obtained from the crystal structure of calpain (*32*, *33*), provide strong evidence that ALG-2 dimerizes via the C-terminal domain of the protein. On the basis of the sequence similarity of ALG-2 and the calpain small subunit, we suggest that the fifth EF-hand Ca^{2+}-binding motif is the actual contact area of the dimer (see the Discussion for more details).

Ca^{2+}-Induced Conformational Changes Inherent to ALG-2. Several experimental approaches were used in investigating the Ca^{2+} binding properties and associated ion-induced conformational changes intrinsic to ALG-2. Because of the low solubility of the Ca^{2+}-bound form of ALG-2, we were only able to study the Ca^{2+} binding of the full-length protein using fluorescence spectroscopy. Incremental additions of Ca^{2+} progressively quenched the intrinsic fluorescence of ALG-2 (Figure 6A). One can also observe a slight red shift of the fluorescence spectra of the protein upon addition of Ca^{2+} (Figure 6A). Large decreases in fluorescence intensity were observed when micromolar concentrations of Ca^{2+} were added to soluble samples of ALG-2. This finding is indicative of the existence of strong Ca^{2+}-binding site(s) of the protein (K_d in the micromolar range). Quenching of the sample's intrinsic fluorescence continued via the addition of Ca^{2+} to the sample preparation up to and exceeding Ca^{2+} concentrations of as high as 10 mM. This phenomenon is indicative of proteins which contain weak Ca^{2+}-binding sites possessing K_d values in the millimolar range. Due to the lack of definitive data which pertain to the Ca^{2+}-binding sites of recombinant ALG-2, it was not possible to derive quantitative K_d values of Ca^{2+} binding based on the data depicted in Figure 6A.

Sequence analysis between ALG-2 and other members of its subfamily revealed that Ca^{2+}-binding sites 1 and 3 of

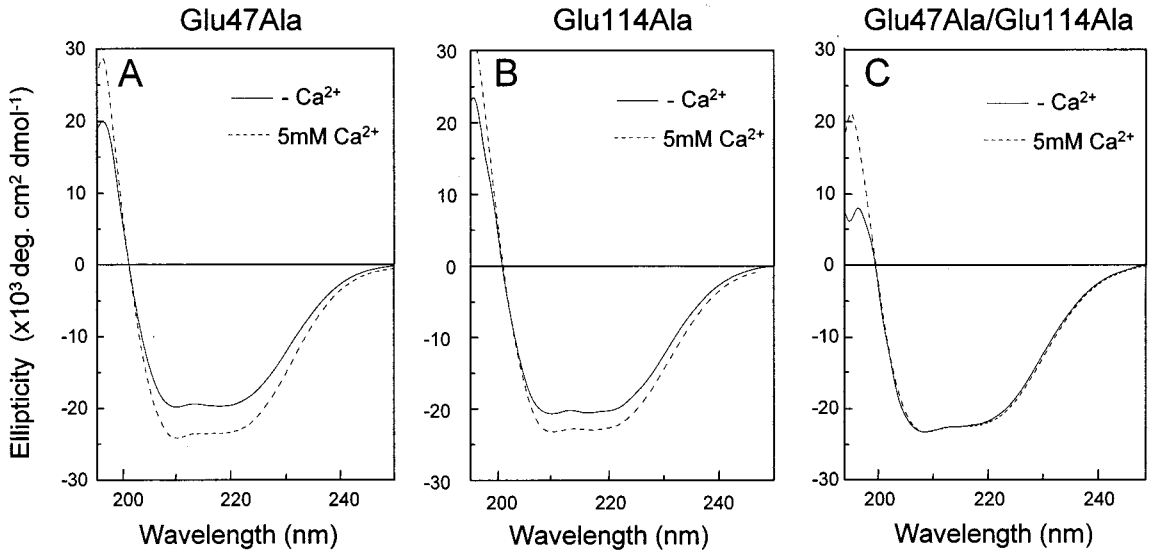

FIGURE 7: Circular dichroism spectra of the Glu47Ala (A), Glu114Ala (B), and Glu47Ala/Glu114Ala (C) point mutants of ALG-2 in the presence and absence of Ca^{2+}. For clarity, CD spectra at two extreme Ca^{2+} concentrations (0 and 5 mM) are shown in each panel. For the two single-point mutants, the spectral change could be observed with the addition of a micromolar concentration of Ca^{2+}. The protein concentration used for the CD measurements was 5 μM for all three samples.

ALG-2 contain the canonical amino acid sequence reported for other EF-hand Ca^{2+}-binding proteins (Figure 1A,B). The other three predicted Ca^{2+}-binding sites within the protein have mutations or insertions at critical positions which are highly conserved among numerous EF-hand Ca^{2+}-binding proteins (*34*−*36*). On this basis, we postulated that the predicted Ca^{2+}-binding sites denoted as sites 1 and 3 correspond to functionally strong Ca^{2+}-binding sites present in ALG-2. Refolded, purified ALG-2-NT requires submicromolar Ca^{2+} concentrations to maintain its structure in solution (data not shown), which suggests that the N-terminal domain contains at least one strong Ca^{2+}-binding site. ALG-2-CT displayed an intrinsic fluorescence intensity quenching similar to that observed for wild-type ALG-2 in response to Ca^{2+} titration (Figure 6B). In contrast to the full-length protein, ALG-2-CT does not undergo a Ca^{2+}-induced aggregation (data not shown). Therefore, the Ca^{2+}-induced Trp fluorescence changes are representative of the conformational changes of the domain. This result also suggests that the C-terminal domain also contains a strong Ca^{2+}-binding site(s). To further prove that sites 1 and 3 correspond to the strong Ca^{2+}-binding sites, we mutated the Glu residue at position 12 of the respective Ca^{2+}-binding loop in the following manner: (i) single mutants Glu47Ala and Glu114Ala and (ii) double mutant Glu47Ala/Glu114Ala (see Figure 1). All three mutants retained their wild-type conformation in the absence of Ca^{2+}, as determined by CD spectroscopy (Figures 4 and 7). Mutation of the 12th Glu residue to Ala within both Ca^{2+}-binding loops of the protein completely disrupted the Ca^{2+}-binding capacity of the mutants. Furthermore, this double mutant lacked the Ca^{2+}-induced precipitation profile characteristic of the wild-type protein even at a Ca^{2+} concentration as high as 20 mM (data not shown). Additionally, CD experiments showed that the addition of Ca^{2+} does not induce detectable conformational changes within the double mutant (Figure 7C). The chemical cross-linking experiment demonstrated that the double mutant has furthermore lost its ability to aggregate in the presence of Ca^{2+} (Figure 8). In contrast, the two single mutants displayed

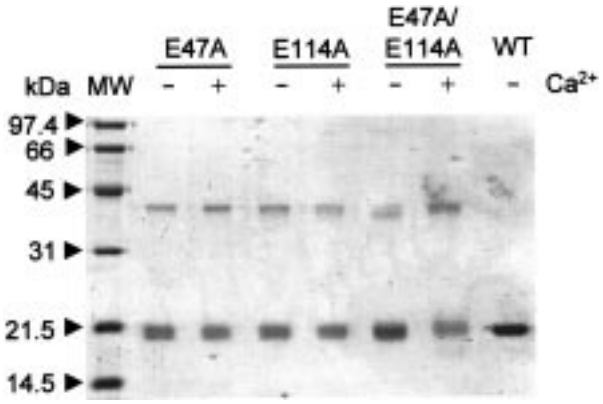

FIGURE 8: Chemical cross-linking of the Ca^{2+}-binding site point mutants in the presence (+) and absence (−) of Ca^{2+}. The wild-type ALG-2 (WT) was used as the molecular mass marker for the monomeric ALG-2.

the well-known Ca^{2+}-induced increases in helicity as previously reported for numerous other EF-hand Ca^{2+}-binding proteins. Disruption of Ca^{2+}-binding site 1 (as achieved with the Glu47Ala mutant of ALG-2) did not lead to any apparent modulation of the protein's propensity to bind Ca^{2+} at sites located within the C-terminus. This was clearly demonstrated in studies that documented the mutant's ability to undergo typical Ca^{2+}-induced negative ellipticity increases at 222 and 208 nm of its far-UV CD spectra (Figure 7A). Similarly, abolishment of the Ca^{2+}-binding capacity of site 3 (via a Glu114Ala mutation of the wild type) did not significantly alter the Ca^{2+} binding property of site 1 (Figure 7B). However, both point mutants displayed variances between themselves and the wild-type protein with respect to their conformational profiles as a result of structural changes induced by Ca^{2+} binding. As expected, both point mutants retained their native conformation in the absence of Ca^{2+} (Figure 7), as the side chain of the 12th Glu residue in Ca^{2+}-binding loops is not predicted to be involved in any interactions with other residues (*38*−*40*). Chemical cross-linking experiments showed that neither of the single mutants underwent Ca^{2+}-induced aggregation, suggesting that both

Ca^{2+}-binding sites are required for the Ca^{2+}-induced conformational change of the proteins (Figure 8). Taken together, we conclude that Ca^{2+}-binding sites 1 and 3 possess strong, apparently independent Ca^{2+}-binding activities.

DISCUSSION

In this work, we have successfully expressed ALG-2 and its various point mutants in their respective soluble forms in bacterial cells at a very high yield. Large quantities of pure ALG-2 (~100 mg/L of bacterial culture) could be easily obtained within 2 days using the purification procedure developed in this work. Additionally, we were also able to express and purify large quantities of the N- and C-terminally truncated mutants of ALG-2 in the same bacterial system. The development of the efficient expression and purification method has laid a foundation as well as provides the means for furthering the biochemical and structural characterization of this novel Ca^{2+}-binding protein implicated for its role in apoptosis.

As shown by the chemical cross-linking experiment, Ca^{2+}-free ALG-2 has a tendency to form a homodimer in solution (Figure 3B). Formation of a homodimer is a common feature for every known member of this subfamily of Ca^{2+}-binding proteins, specifically, sorcin, grancalcin, and the calpain small subunit (*28*−*33*). In these studies, it has been shown, utilizing several trucated mutants of the protein, that the dimerization region of ALG-2 is likely to be located within the C-terminal region. A combination of amino acid sequence analysis and mutagenesis studies allowed us to identify Lys137 in ALG-2 as the specific cross-linking site which gives rise to the formation of the dimer complex. Together with the crystal structure of the calpain small subunit, we suggest that ALG-2 may form a homodimer by packing together the fifth EF-hands from each monomer (*32*, *33*). However, a definitive answer for the dimerization interface awaits the determination of the three-dimensional structure of the protein. In the absence of Ca^{2+}, the association between the ALG-2 monomers is much weaker than those observed for other members of the subfamily. Gel filtration experiments showed that Ca^{2+}-free ALG-2 exists predominantly as a monomer in solution (Figure 2A), whereas sorcin, grancalcin, and the calpain small subunit all form stable dimers under similar conditions (*28*−*33*). The crystal structures of the calpain small subunit show that the fifth EF-hand of each monomer forms a four-helix bundle dimer interface, and the interactions between the monomer are mediated primarily by packing the hydrophobic amino acid residues between these two EF-hand motifs (*32*, *33*). Sequence alignment indicates that the hydrophobic amino acid residues in the fifth EF-hand of ALG-2 and calpain are highly conserved (Figure 1A). Thus, it is difficult to explain the affinity difference between the monomers of ALG-2 and other members of the subfamily without a detailed atomic structure of the protein. Studies have recently been initiated in our laboratory to determine the solution structure of ALG-2 by NMR spectroscopy.

Since the expression level of ALG-2 has been reported to remain constant during apoptosis, it was proposed that ALG-2 is likely to exert its function through a Ca^{2+}-dependent mechanism (*25*). Thus, knowledge of Ca^{2+} binding properties and Ca^{2+}-induced conformational changes is critical for understanding the function of ALG-2 within the cellular environment. Sequence alignment shows that the Ca^{2+}-binding sites of ALG-2 display significant differences with the corresponding sites in other members of the family (Figure 1). Specifically, Ca^{2+}-binding site 1 of ALG-2 contains the conserved sequence determinants necessary for Ca^{2+} binding (*34*−*37*; Figure 1B), and it is likely to be a strong Ca^{2+}-binding site. Indeed, mutation of the Glu residue at position 12 of the Ca^{2+}-binding loop to an Ala drastically altered the Ca^{2+}-binding property of the protein (Figures 7 and 8). In contrast, Ca^{2+}-binding sites 1 of the other three members of the family all contain a novel 11-residue Ca^{2+}-binding loop with the *X* coordinate provided by the main chain carbonyl oxygen of an Ala residue (*32*, *33*). Despite significant sequence differences, Ca^{2+}-binding sites 1 of both ALG-2 and calpain are able to bind to Ca^{2+} with a high affinity (ref *33* and this study). Ca^{2+}-binding sites 3 of ALG-2 and other members of the family all contain highly conserved amino acid residues observed in canonical EF-hand Ca^{2+}-binding proteins (Figure 1A,B). Like that for calpain (*32*), Ca^{2+}-binding site 3 of ALG-2 is likely to be a strong Ca^{2+}-binding site as indicated by the truncation and mutation studies of the protein. The X-ray crystal structures have shown that Ca^{2+}-binding site 2 of calpain also binds to Ca^{2+} with a high affinity, and the result is within the expectation as the particular Ca^{2+}-binding loop contains all the necessary amino acids required for strong Ca^{2+} binding (*32*; see also Figure 1). In contrast, the amino acid residue in the sixth position of the second Ca^{2+}-binding site of ALG-2 is an Ala rather than the highly conserved Gly (*41*). Formation of pentagonal bipyramidal coordination of Ca^{2+} is facilitated by an unusual main chain conformation (ϕ and $\psi \sim 60°$ and 20°, respectively) of this particular Gly residue (*42*), and such Gly to Ala substitution is likely to reduce the Ca^{2+}-binding affinity of the site dramatically. Ca^{2+}-binding site 4 of ALG-2 is also very different from site 4 of calpain, sorcin, and grancalcin. In ALG-2, the 12th position of the loop is an Asp rather than a Glu residue. Mutation of the bidentate Glu residue at this position is known to drastically reduce the Ca^{2+}-binding affinity of EF-hand Ca^{2+}-binding proteins (*43*, *44*). Therefore, Ca^{2+}-binding site 4 of ALG-2 is also likely to be a weak one, although the coordination sphere of this Ca^{2+}-binding site is expected to be similar to the one in the canonical Ca^{2+}-binding site. The crystal structures of calpain showed that site 4 of the protein binds to Ca^{2+} only at a physiologically irrelevant Ca^{2+} concentration, and uniquely, all of the Ca^{2+} ligands are provided by amino acid residues in the F-helix of the EF-hand (*32*, *33*). An insertion of a hydrophobic amino acid residue between the seventh and eighth positions of the fifth Ca^{2+}-binding site of ALG-2 as well as other members of the family will likely abolish the Ca^{2+}-binding capacity of the site. The crystal structures of calpain have indeed revealed that the fifth Ca^{2+}-binding site remains unoccupied even when 200 mM Ca^{2+} was included in the crystallization buffer, and the two helices of the EF-hand are nearly antiparallel with each other (*32*, *33*, *38*−*40*).

In this work, we also showed that ALG-2 can be divided into two folded domains at Thr93 (Figure 4). The result indicates that the first two Ca^{2+}-binding sites are likely to be independent of the three C-terminal Ca^{2+}-binding sites. It was further shown that the N-terminal domain of ALG-2 could still bind to Ca^{2+} when the C-terminal Ca^{2+}-binding

site was mutated (Figure 7B). Similarly, "knock-out" of the N-terminal Ca^{2+}-binding site did not impair the Ca^{2+} binding of the C-terminal domain (Figure 7A). The data can readily be explained by the crystal structure of calpain (*32*, *33*). The first two EF-hands of the calpain small subunit pack with each other, forming a relatively independent structural unit, and Ca^{2+}-binding motifs 3 and 4 form another pair of EF-hands, leaving the fifth EF-hand to pair with the same section from the other monomer. From the crystal structure, one does not expect a significant amount of communication between the Ca^{2+}-binding sites of the two domains. The lack of communication between the Ca^{2+}-binding sites was previously demonstrated experimentally for calpain (*45*).

Ca^{2+}-induced conformational changes of ALG-2 were studied by a number of approaches. Both chemical cross-linking and gel filtration experiments showed that ALG-2 undergoes a Ca^{2+}-induced aggregation (Figure 3), presumably as a result of conformational changes of the protein. It was observed previously that sorcin also undergoes a Ca^{2+}-induced aggregation (*29*), and calcium was shown to be required for the binding of sorcin to synexin (*46*), and translocation of the protein from cytosol to cellular membranes (*47*). It is likely that binding of Ca^{2+} to ALG-2 and sorcin leads to an exposure of their respective hydrophobic surfaces. In the absence of their respective targets, both proteins undergo self-aggregation via their respective hydrophobic surfaces (*49*). Inside cells, however, ALG-2 may interact with its target proteins in a Ca^{2+}-dependent manner. It was reported that ALG-2 binds with another Ca^{2+}-binding protein highly homologous to ALG-2 itself (*48*). It is quite possible that ALG-2 binds to this Ca^{2+}-binding protein using its fifth EF-hand motif. The significant conformational changes of ALG-2 upon binding to Ca^{2+} are also manifested by a large decrease (~60%) of the intrinsic Trp fluorescence intensity of the protein (Figure 6A). The quenching of the intrinsic fluorescence may reflect a significant change of the microenviroment of the Trp residues of the protein. The other possibility of the observed fluorescence quenching may result from the Ca^{2+}-induced aggregation of the protein. Since a similar fluorescence quenching was also observed for ALG-2-CT, ALG-2-CT does not aggregate upon addition of Ca^{2+}. The conformational change is likely to be the main origin of the Ca^{2+}-induced fluorescence quenching of the full-length ALG-2.

The Ca^{2+}-induced conformational changes of ALG-2 were further investigated using the fragments and Ca^{2+}-binding site mutants of the protein. Like that of the full-length protein, the intrinsic Trp fluorescence of ALG-2-CT was quenched upon binding to Ca^{2+} (Figure 6B), indicating a conformational change of the C-terminal part of the protein. The Ca^{2+}-induced conformational changes in the C-terminal domain are further supported by the CD spectra of the Glu47Ala mutant of the protein (Figure 7A). The substitution of Glu47 with an Ala abolished Ca^{2+} binding to the N-terminal domain of the protein. Therefore, the increase of the α-helicity upon addition of Ca^{2+} to the mutant ALG-2 likely resulted from the conformational changes of the C-terminal domain. Removal of Ca^{2+} resulted in an immediate precipitation of ALG-2-NT (data not shown), indicating that the conformation of the N-terminal part of the protein is also sensitive to Ca^{2+}. The CD results of the Glu114Ala mutant shown in Figure 7B also indicated that the N-terminal domain of ALG-2 experiences a Ca^{2+}-induced conformational change. Furthermore, Ca^{2+}-induced conformational changes originate solely from the binding of Ca^{2+} to the two strong sites (sites 1 and 3) of the protein. This finding is further supported by the fact that mutation of these two sites resulted in an ALG-2 mutant whose conformation integrity is entirely independent of Ca^{2+} (Figure 7C).

The Glu47Ala/Glu114Ala double mutant of ALG-2 generated in this work has completely lost its Ca^{2+}-binding capacity (Figure 7C). This mutant may be particularly useful in addressing the in vivo functioning of ALG-2. Additionally, it is plausible that this mutant may provide insight into the ability of Ca^{2+} to regulate ALG-2 in vivo by comparing the apoptotic response of cells transfected with the wild type as compared to that of the mutant form. Furthermore, this double mutant could also serve as a dominant negative of ALG-2 for studying the cellular function of the protein as well as its signaling pathway.

In summary, an efficient purification method was developed for isolating large quantities of recombinant ALG-2 from bacterial cells. ALG-2 contains five EF-hand Ca^{2+}-binding sites. It is a new member of the calpain small subunit subfamily Ca^{2+}-binding protein. The protein forms a weak dimer in solution, and the dimer interface is likely to be formed by the fifth EF-hand of the protein. The protein undergoes a significant Ca^{2+}-induced conformational change, and such conformational change may be directly related to the protein's functional regulation.

ACKNOWLEDGMENT

We thank Dr. David Miller-Martini for critical reading of and comments on the manuscript.

REFERENCES

1. Jacobson, M. D., Weil, M., and Raff, M. C. (1997) *Cell 88*, 347−354.
2. Green, D. R. (1998) *Cell 94*, 695−698.
3. Ashkenazi, A., and Dixit, V. M. (1998) *Science 281*, 1305−1308.
4. Thornberry, N. A., and Lazebnik, Y. (1998) *Science 281*, 1312−1316.
5. Adams, J. M., and Cory, S. (1998) *Science 281*, 1322−1326.
6. Yuan, J., Shaham, S., Ledoux, S., Ellis, H. M., and Hoevitz, H. R. (1993) *Cell 75*, 641−652.
7. Yuan, J., and Hoevitz, H. R. (1990) *Dev. Biol. 138*, 33−41.
8. Hengartner, M. O., Ellis, R. E., and Horvitz, H. R. (1992) *Nature 356*, 494−499.
9. Minn, A. J., Velez, P., Schendel, S. L., Liang, H., Muchmore, S. W., Fesik, S. W., Fill, M., and Thompson, C. B. (1997) *Nature 385*, 353−357.
10. Schendel, S. L., Xie, Z., Montal, M. O., Matsuyama, S., Montal, M., and Reed, J. C. (1997) *Proc. Natl. Acad. Sci. U.S.A. 94*, 5113−5118.
11. Antonsson, B., Conti, F., Ciavatta, A., Montessuit, S., Lewis, S., Martinou, I., Bernasconi, L., Bernard, A., Mermod, J. J., Mazzei, G., Maundrell, K., Gambale, F., Sadoul, R., and Martinou, J. C. (1997) *Science 277*, 370−372.
12. Lam, M., Bhat, M. B., Nuñez, G., Ma, J., and Distelhorst, C. W. (1998) *J. Biol. Chem. 273*, 17307−17310.
13. Baffy, G., Miyashita, T., Williamson, J. R., and Reed, J. C. (1993) *J. Biol. Chem. 268*, 6511−6519.
14. He, H., Lam, M., McCormick, T. S., and Distelhorst, C. W. (1997) *J. Cell Biol. 138*, 1219−1228.
15. Nicotera, P., and Orrenius, S. (1998) *Cell Calcium 23*, 173−180.

16. Murphy, A. N., Bredesen, D. E., Cortopassi, G., Wang, E., and Fiskum, G. (1996) *Proc. Natl. Acad. Sci. U.S.A. 93*, 9893−9898.
17. Zamzami, N., Susin, S. A., Marchetti, P., Hirsh, T., Gomez-Monterrey, I., Castedo, M., and Kroemer, G. (1996) *J. Exp. Med. 183*, 1533−1544.
18. Shimizu, S., Eguchi, Y., Kamiike, W., Funahashi, Y., Mignon, A., Lacronique, V., Matsuda, H., and Tsujimoto, Y. (1998) *Proc. Natl. Acad. Sci. U.S.A. 95*, 1455−1459.
19. Trump, B. F., and Berezesky, I. K. (1995) *FASEB J. 9*, 219−228.
20. Kaiser, N., and Edelman, I. S. (1977) *Proc. Natl. Acad. Sci. U.S.A. 74*, 638−642.
21. Kaiser, N., and Edelman, I. S. (1978) *Endocrinology 103*, 936−942.
22. Jiang, S., Chow, S. C., Nicotera, P., and Orrenius, S. (1994) *Exp. Cell Res. 212*, 84−92.
23. McConkey, D. J., Nicotera, P., Hartzell, P., Bellomo, G., Wyllie, A. H., and Orrenius, S. (1989) *Arch. Biochem. Biophys. 269*, 365−370.
24. Dowd, D. R., MacDonald, P. N., Komm, B. S., Haussler, M. R., and Miesfeld, R. L. (1992) *Mol. Endocrinol. 6*, 1843−1848.
25. Vito, P., Lacanà, E., and D'Aamio, L. (1996) *Science 271*, 521−525.
26. Lacanà, E., Ganjei, J. K., Vito, P., and D'Aamio, L. (1997) *J. Immunol. 158*, 5129−5135.
27. Mikaelian, I., and Sergeant, A. (1992) *Nucleic Acids Res. 20*, 376.
28. Hamada, H., Okochi, E., Oh-hara, T., and Tsuruo, T. (1988) *Cancer Res. 48*, 3173−3178.
29. Zamparelli, C., Ilari, A., Verzili, D., Vecchini, P., and Chiancone, E. (1997) *FEBS Lett. 409*, 1−6.
30. Teahan, C. G., Totty, N. F., and Segal, A. W. (1992) *Biochem. J. 286*, 549−545.
31. Blanchard, H., Li, Y., Cygler, M., Kay, C. M., Arthur, J. S. C., Davies, P. L., and Elce, J. S. (1996) *Protein Sci. 5*, 535−537.
32. Blanchard, H., Grochulski, P., Li, Y., Arthur, J. S. C., Davies, P. L., Elce, J. S., and Cygler, M. (1997) *Nat. Struct. Biol. 4*, 532−538.
33. Lin, G., Chattopadhyay, D., Maki, M., Wang, K. K. W., Carson, M., Jin, L., Yuen, P., Takano, E., Hatanaka, M., DeLucas, L. J., and Narayana, S. V. L. (1997) *Nat. Struct. Biol. 4*, 539−547.
34. Renner, M., Danielson, M. A., and Falke, J. J. (1993) *Proc. Natl. Acad. Sci. U.S.A. 90*, 6493−6497.
35. Kawasaki, H., and Kretsinger, R. H. (1995) *Protein Profile 2*, 305−490.
36. Linse, S., and Forsén, S. (1995) *Adv. Second Messenger Phosphoprotein Res. 30*, 89−151.
37. Marsden, B. J., Shaw, G. S., and Sykes, B. D. (1990) *Biochem. Cell. Biol. 68*, 587−601.
38. Zhang, M., Tanaka, T., and Ikura, M. (1995) *Nat. Struct. Biol. 2*, 758−767.
39. Kuboniwa, H., Tjandra, N., Grzesiek, S., Ren, H., Klee, C., and Bax, A. (1995) *Nat. Struct. Biol. 2*, 768−776.
40. Finn, B. E., Evenas, J., Drakenberg, T., Waltho, J. P., Thulin, E., and Forsén, S. (1995) *Nat. Struct. Biol. 2*, 777−783.
41. Drake, S., Zimmer, M. A., Miller, C. L., and Falke, J. J. (1997) *Biochemistry 36*, 9917−9926.
42. Strynadka, N. C. J., and James, M. N. G. (1989) *Annu. Rev. Biochem. 58*, 951−998.
43. Maune, J. F., Bechinham, K., Martin, S. R., and Bayley, P. M. (1992) *Biochemistry 31*, 7779−7786.
44. Carlström, G., and Chazin, W. J. (1993) *J. Mol. Biol. 231*, 415−430.
45. Michetti, M., Salamino, F., Minafra, R., Melloni, E., and Pontremoli, S. (1997) *Biochem. J. 325*, 721−726.
46. Brownawell, A. M., and Creuta, C. E. (1997) *J. Biol. Chem. 272*, 22182−22190.
47. Meyers, M. B., Zamparelli, C., Verzili, D., Dicker, A. P., Blanck, T. J. J., and Chiancone, E. (1995) *FEBS Lett. 357*, 230−234.
48. D'Aamio, L., Lacanà, E., and Vito, P. (1997) *Semin. Immunol. 9*, 17−23.
49. Maki, M., Yamaguchi, K., Kitaura, Y., Satoh, H., and Hitomi, K. (1998) *J. Biochem. 124*, 1170−1177.
50. Thompson, J. D., Higgins, D. G., and Gibson, T. J. (1994) *Nucleic Acids Res. 22*, 4673−4680.
51. Kraulis, P. J. (1991) *J. Appl. Crystallogr. 24*, 946−950.

BI990034N